Comparison of color imaging vs. hyperspectral imaging for texture classification

Alice Porebski, Mohamed Alimoussa, Nicolas Vandenbroucke

Comparison of Color Imaging vs. Hyperspectral Imaging for Texture Classification

Alice Porebski Mohamed Alimoussa
Nicolas Vandenbroucke
Univ. Littoral Côte d'Opale, UR 4491, LISIC, Calais, F-62100, France

2 August 2022

Abstract

Many approaches of texture analysis by color or hyperspectral imaging are based on the assumption that the image of a texture can be viewed as a multi-component image, where spatial interactions within and between components are jointly considered (opponent component approach) or not (marginal approach). When color images are coded in multiple color spaces, texture descriptors are based on Multi Color Channel (MCC) representations. By extension, a Multi Spectral Band (MSB) representation can be used to characterize the texture of material surfaces in hyperspectral images. MSB and MCC representations are compared in this paper for texture classification issues. The contribution of each representation is investigated with marginal and/or opponent component strategies. For this purpose, several relevant texture descriptors are considered. Since MSB and MCC representations generate high-dimensional feature spaces, a dimensionality reduction is applied to avoid the curse of dimensionality. Experimental results carried out on three hyperspectral texture databases (HyTexiLa, SpecTex and an original dataset extracted from the Timbers database) show that considering between component interactions in addition to the within ones significantly improves the classification accuracies. The proposed approaches allow also to outperform state of the art hand-designed descriptors and CNN-based color texture descriptors. This study highlights the contribution of hyperspectral imaging compared to color imaging for texture classification purposes but also the advantages of color imaging depending on the considered texture representation.

1 Introduction

Texture and color are two salient visual cues of human vision. They provide useful information in identifying objects or regions of interest in images. Texture analysis has attracted extensive research attention over the last fifty years. Many descriptors have been defined to represent the texture in an image, from hand-designed descriptors like co-occurrence matrices introduced by Haralick in 1973 to more recent CNN-based methods, by way of well known Local Binary Patterns (LBP) [1, 2]. Most descriptors have initially been hand-designed to represent textures in gray-level images, by evaluating the spatial distribution of gray-levels in a neighborhood. Many have then been extended to color, based on the assumption that texture and color information can be combined either separately or jointly, especially for color texture classification applications, where an image has to be assigned to a class among different categories [3].

The color information is initially coded by the three color channels of the RGB color space, and can also be transformed in several other three-dimensional color spaces [4]. Recently, multi color space approaches have emerged to characterize the color tex-

ture in images [5, 6, 7]. These approaches select color texture features from descriptors that are computed from images coded in different color spaces, leading to a Multi Color Channel (MCC) representation [8]. In this context, a texture is viewed as a multi component image, where the components correspond to the channels of the considered color spaces. By exploiting the properties of several color spaces simultaneously, the MCC representation takes advantage of the discrimination quality of different color spaces and avoids the difficulty of choosing a relevant color space, since it depends on the considered application.

In the same way, texture analysis in hyperspectral images has also attracted research attention. Hand-designed texture descriptors, like co-occurence matrices or LBP, have been extended to analyze the spectral characteristics of the texture of materials [9, 10, 11]. Each pixel of a hyperspectral image represents the reflectance spectrum of the corresponding observed surface, so that a texture can be viewed as a multi component image where the components correspond to the spectral bands identified by their wavelength. In this context, texture is characterized thanks to a Multi Spectral Band (MSB) representation, by extension to the MCC one [8].

MCC and MSB both generate a high-dimensional space and generally require dimensionality reduction to avoid the curse of dimensionality [5, 9, 12]. Figure 1 illustrates an unified representation of these two approaches to describe textures thanks to color or hyperspectral imaging.

Here MSB and MCC representations will be compared for texture classification purposes. In [8], an initial MSB and MCC comparison has already been undertaken by considering only within-component interactions to describe textures with marginal descriptors. In this paper, we will investigate the contribution of each approach taking within and between-component interactions into account with opponent component descriptors. For this purpose, several relevant texture descriptors are considered. For a fair comparison, the dimension of the feature spaces obtained by MSB and MCC will be reduced by using a unified embedded feature selection model. Experimental results will be analyzed on three hyperspectral texture databases (HyTexiLa, SpecTex and an original dataset extracted from the Timbers database) and compared with recent hand-designed and CNN-based color texture descriptors.

The second section of this paper presents how color and spectral texture features are computed from color and hyperspectral images respectively. The third section details the feature selection schemes considered to represent textures in a reduced dimensionality feature space. Finally, in the fifth section, experimental results obtained with MSB and MCC representations are compared each other and with state of the art hand-designed and CNN-based descriptors, based on the experimental conditions presented in the fourth section. In this section, experiments are carried out on two benchmark hyperspectral texture datasets and a challenging dataset is introduced to assess the classification performance.

2 Color and spectral texture features

Numerous researchers have proposed a large number of effective texture feature extracting methods [1]. These methods can be divided into two categories depending on the texture descriptors are hand-designed (theory-driven representation) or directly designed from the data (data-driven representation) [2]. The data-driven representation includes CNN-based texture features and the theory-driven representation can be classified into global descriptors, like co-occurrence matrices [13], from which statistics are extracted to characterize the texture, and local descriptors, like LBP [14], from which histograms are computed to represent the texture [15]. Since the introduction of LBP by Ojala in 1996 for gray-level images, a large number of LBP variants may be found in the literature, like Local Ternary Pattern (LTP), Completed LBP (CLBP), Median Robust Extended LBP (MRELBP) and so on [16]. Most of these approaches have been developed for gray-level images and do not take into account the correlation information among multiple color channels or spectral bands [17]. Many hand-designed descriptors have then been extended to color, like co-occurrence matrices which

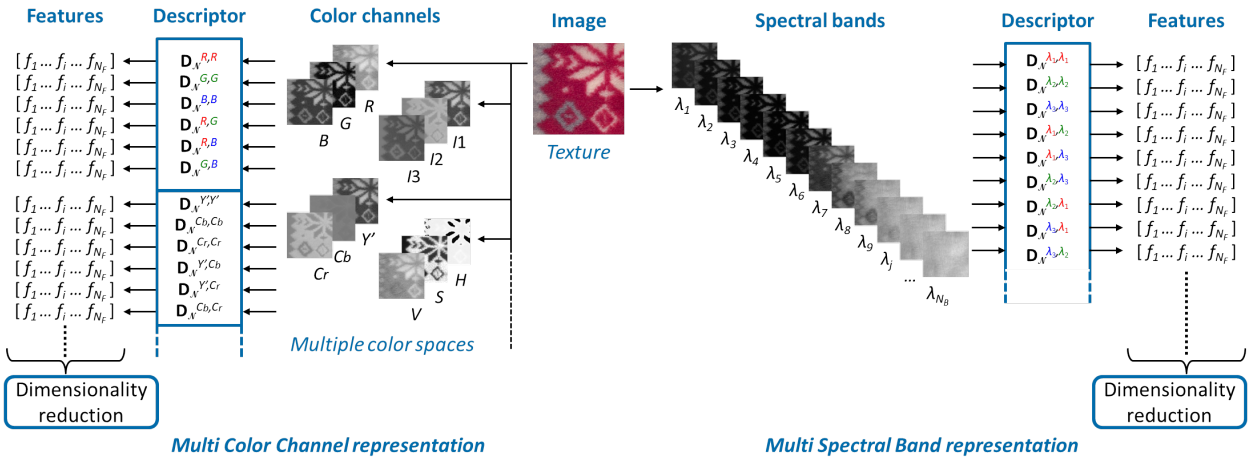

Figure 1: Illustration of MCC and MSB representations.

have been extended by Palm in 2004 to define the Integrative Co-occurence Matrices (ICM) [18], or LBP which have been extended to Opponent Color LBP (OCLBP) [3].

This extension to color can generally be done according to three main strategies that jointly consider spatial and color information: the marginal strategy (Mar), where the color texture descriptors take into account the spatial relationships within each of the three color channels of the used color space; the opponent strategy (Opp), where the spatial relationships between each of the three color channels are considered; and the marginal + opponent strategy (Mar+Opp), where within and between channel interactions are exploited. Recently, several descriptors that simultaneously consider more than two color channels to characterize the textures have emerged, like Hybrid Color LBP (HCLBP) [19], LBP for Color images (LBPC) [20], Spatially Weighted Order Binary Pattern (SWOBP) [21], Quaternionic extended LBP (QxLBP) [22] and Multiple Channels LBP (MCLBP) [17]. However, to investigate the contribution of MSB and MCC representations, we have focused our interest on descriptors that can be applied in the Mar, Opp and Mar+Opp strategies: ICM [18], LBP [3], Improved LBP (ILBP) [23] and Local Color Vector Binary Patterns (LCVBP) [24]. The extension to color of a descriptor X can thus lead to three MCC representations (MCC-X-Mar, MCC-X-Opp and MCC-X-Mar+Opp) or three MSB representations (MSB-X-Mar, MSB-X-Opp and MSB-X-Mar+Opp).

In a MCC representation, a color image is coded in N_C color spaces simultaneously, whereas in a MSB representation, a hyperspectral image is considered as a set of N_B spectral band images identified by their wavelengths. For these two representations, the texture is characterized by a set of D texture features depending on the considered hand-designed texture descriptors described in the next sections. The goal of this paper being to compare the MSB and MCC representations each other and with hand-designed and CNN-based descriptors of the state of the art, we choose to consider a standard and unified setting for descriptors which need to define a neighborhood, like ICM or LBP-based descriptors. In [25], it has been shown that the choice of neighborhood directions depends on the texture orientation. The hyperspectral databases here used do not present textures with a specific orientation. For this reason, 8 neighbor pixels oriented toward 0°, 45°, 90°, 135°, 180°, 225°, 270°, 315° and 1 pixel radius are here considered.

The following sections present the texture descriptors used in MCC and MSB representations. Please

refer to Table 1 to have the feature space dimension D obtained with each descriptor.

2.1 Marginal texture descriptors (Mar)

Marginal Integrative Co-occurrence Matrices (ICM-Mar) 14 Haralick features (energy, homogeneity, contrast, correlation, variance, inverse difference moment, sum average, sum entropy, entropy, difference variance, difference entropy, two measures of correlation I and II, and maximal correlation coefficient [13]) are computed from reduced size chromatic co-occurrence matrices extracted from each color channel or spectral band separately as described in [8]. A reduced size chromatic co-occurrence matrix is a $Q \times Q$ co-occurrence matrix, where the quantization level Q is reduced in order to decrease the memory storage cost and so, the time required to extract texture features from these matrices [26].

Marginal Local Binary Pattern (LBP-Mar) (256)-dimensional LBP histograms are extracted from each color channel or spectral band separately as described in [27, 8].

Marginal Improved Local Binary Pattern (ILBP-Mar) (511)-dimensional ILBP histograms are extracted from each color channel or spectral band separately. In LBP, the neighbor pixels are thresholded with the value of the central pixel to give a binary number, whereas in ILBP, thresholding is done with the average value of the neighbor pixels [23].

2.2 Opponent texture descriptors (Opp)

Local Color Vector Binary Patterns (LCVBP-Opp) Lee et al. propose to characterize textures by concatenating one (256)-dimensional Color Norm Pattern (CNP) histogram and three (256)-dimensional Color Angular Pattern (CAP) histograms [24]. The CNP histogram is derived from the norm of color pixel values and the CAP histograms are derived from the ratio of pixel values between pairs of color channels. We propose to only consider the CAP histograms extracted from each pair of spectral bands or color channels within each considered color space.

2.3 Marginal + opponent texture descriptors (Mar+Opp)

Marginal + opponent Integrative Co-occurrence Matrices (ICM-Mar+Opp) 14 co-occurrence features are extracted from each color channel or spectral band separately, and from each pair of spectral bands or color channels within each considered color space. The considered Haralick features are the same as in ICM-Mar (see Section 2.1).

Marginal + opponent Local Binary Pattern (LBP-Mar+Opp) (256)-dimensional LBP histograms are extracted from each color channel or spectral band separately, and from each pair of spectral bands or color channels within each considered color space.

Marginal + opponent Improved Local Binary Pattern (ILBP-Mar+Opp) (512)-dimensional ILBP histograms [23] are extracted from each color channel or spectral band separately, and from each pair of spectral bands or color channels within each considered color space.

3 Dimensionality reduction

Supervised texture classification aims to assign a texture to one of a set of predefined categories for which training samples are available. This process is divided into two successive stages: a learning stage in which a classifier is trained with labeled training samples and a decision stage where this classifier is evaluated with a testing set in order to measure its ability to predict the class labels of new samples.

MCC and MSB representations take into account numerous properties of texture but they tend to produce a large and sometimes redundant amount of fea-

Table 1: Feature space dimension D obtained with MCC and MSB representations, according to the used descriptor.

Descriptor	Feature space dimension D
MCC-ICM-Mar	$N_C \times 3$ (channels) $\times$ 14 (statistics)
MSB-ICM-Mar	$N_B \times 14$ (statistics)
MCC-LBP-Mar	$N_C \times 3$ (channels) $\times$ (256-dimensional histograms)
MSB-LBP-Mar	$N_B \times$ (256-dimensional histograms)
MCC-ILBP-Mar	$N_C \times 3$ (channels) $\times$ (511-dimensional histograms)
MSB-ILBP-Mar	$N_B \times$ (511-dimensional histograms)
MCC-LCVBP-Opp	$N_C \times 3$ (pairs) $\times$ (256-dimensional histograms)
MSB-LCVBP-Opp	$1/2 \times N_B \times (N_B - 1) \times$ (256-dimensional hist.)
MCC-ICM-Mar+Opp	$N_C \times$ [3 (channels) + 3 (pairs)] $\times$ 14 (statistics)
MSB-ICM-Mar+Opp	$1/2 \times N_B \times (N_B + 1) \times 14$ (statistics)
MCC-LBP-Mar+Opp	$N_C \times$ [3 (channels) + 6 (pairs)] $\times$ (256-dim. hist.)
MSB-LBP-Mar+Opp	${N_B}^2 \times$ (256-dimensional histograms)
MCC-ILBP-Mar+Opp	$N_C \times$ [3 (channels) + 3 (pairs)] $\times$ (512-dim. hist.)
MSB-ILBP-Mar+Opp	$1/2 \times N_B \times (N_B + 1) \times$ (512-dimensional hist.)

tures, especially when the number of color channels or spectral bands is high. It is well-known that the dimension of the feature space impacts the classification performances due to the curse of dimensionality [28]. Dimensionality reduction methods are thus generally applied to reach satisfying classification accuracies while decreasing memory storage and computation time [29]. This reduction can be achieved during the learning stage either by feature extraction or by feature selection schemes. The latter ones are usually preferred since feature extraction leads to a change of the original feature space semantic and explainability. Moreover, since it requires the computation of the initial feature set to obtain the new reduced feature space, it could be time consuming. Three main models are generally considered for feature selection, depending on the chosen evaluation function: filter, wrapper and embedded [29]. Wrapper model uses the accuracy of a classifier to perform feature selection. It provides good results and easily determines the dimension of the feature subspace but involves an important learning time and classifier-dependent results. Filter model evaluates the discrimination power of different candidate feature sub-spaces without classifying the images. It is less time consuming but suffers to the difficulty to determine the dimension of the feature sub-space to be selected. To obtain a good compromise between dimension determination, computation time and classification result, an embedded model is preferred. It combines a filter model to determine the most discriminating feature sub-spaces at different dimensions and a wrapper one to determine the dimension of the selected sub-space. Moreover, when high dimensional data have to be analyzed, clustering-based selection algorithms are often considered [30]. These approaches divide the initial feature space into a set of groups called clusters, where features of a same group are considered as redundant. They allow to significantly reduce the selection processing time since only one feature per cluster is selected.

In this paper, we propose to consider a supervised embedded feature selection scheme associated with different search procedures and evaluation criteria, depending on the considered texture descriptor:

- When the ICM descriptor is considered, a Clustering-based Sequential Feature Selection (CSFS) procedure is applied with the Wilks's criterion [30] (see section 3.1).
- When LBP, ILBP and LCVBP descriptors are considered, a histogram ranking is performed

with the Intra-Class Separability (ICS) measure as proposed in [5] (see section 3.2).

3.1 Feature selection

To reduce the D-dimensional candidate feature space, the CSFS approach is applied. This approach consists of two stages [30]. Firstly, a dependency graph-based clustering is considered to cluster the feature space. The method uses a correlation coefficient whose threshold is automatically determined by evaluating the feature clustering with a feature separability measure. Secondly, a sequential forward selection approach, based on the Wilks's criterion, is applied to the initial feature space so that a feature is added to the sub-space under construction at each iteration step. Once a feature is selected, features belonging to the same cluster are removed and thus not considered in the next steps. It enables to dramatically reduce the number of candidate features at each step and so the selection processing time. The procedure stops when all the clusters of features are removed.

Once the CSFS approach has determined the most discriminating feature sub-spaces at different dimensions d, the next step of the considered embedded selection scheme consists in measuring the accuracy reached with these sub-spaces to determine the $\hat{d}$-dimensional final relevant feature sub-space. For this purpose, the training set is divided following a k-fold evaluation. $(k-1)$ folds are used to constitute a training image subset and the remaining fold is assigned to a validation image subset from which the classification accuracy is measured.

3.2 Histogram selection

To reduce the candidate space composed of D multi-dimensional histograms, a histogram selection procedure using a ranking algorithm is considered. It consists in computing a score for each histogram in order to measure its relevance to discriminate the considered texture classes. Here, the histogram relevance is evaluated thanks to the ICS-score, which measures the ability of a histogram to similarly represent the textures of a same class [5]. Once the score of each histogram is evaluated, the histograms are ranked in the decreasing order.

Then, the candidate sub-spaces – made up, at the first step, of the histogram with the best score, at the second step, of the two first ranked histograms which are concatenated and so on – are evaluated. As previously, a k-fold evaluation is used to predict the classification accuracy in each concatenated histogram sub-space at each step d. The selected sub-space composed of $\hat{d}$ histograms is the one which maximizes the mean rate of well-classified validation images. Let us note that $\hat{d}$ and D must be multiplied by the number of considered bins to have the final feature space dimension.

4 Experimental conditions

4.1 Considered image datasets

Hyperspectral cameras capture either radiance or reflectance images. The latter can be computed from the radiance data by means of a calibration procedure. In this paper, three datasets of hyperspectral reflectance images have been employed: HyTexiLa, SpecTex and Timbers [10, 31, 32]. To evaluate the MCC representation, each hyperspectral image is transformed to a color image by selecting three spectral band images with wavelength centered on red, green and blue components.

HyTexiLa is a dataset of hyperspectral reflectance images that span the visible (VIS) and near infrared (NIR) parts of the electromagnetic spectrum of 112 textured materials [10]. These 112 texture images represent 112 different classes. Each of these texture images is split into 25 sub-images of size $204 \times 204 \times 27$ where $N_B = 27$ is the number of uniformly distributed spectral bands preselected out of the 186 available ones [8] (see Table 2). Among these 25 sub-images, 12 were randomly considered to be training images and the 13 others as testing images. To evaluate the MCC representation, each one of the 112 reflectance images is transformed to a color image by means of a conversion to the sRGB color space by using the spectral band numbered 65 ($\approx$ 612 nm), 45 ($\approx$ 547 nm), and 18 ($\approx$ 464.5 nm).

Table 2: Summary of image datasets used in experiments.

Dataset	Image size	# classes	# training img./class	# testing img./class	# spectral bands N_B
HyTexiLa	204×204	112	12 (1344)	13 (1456)	27
SpecTex	40×40	60	64 (3840)	192 (11520)	39
Timbers	64×64	3	480 (1440)	480 (1440)	30

SpecTex is a spectral image database including 60 textile samples with different texture patterns [31]. In this paper, we propose to use a downsampled version of the SpecTex database provided by the authors with a spectral sampling of $N_B = 39$ spectral bands out of the 77 available ones [8]. Each of the 60 original images is split up into 256 non-overlapping sub-images leading to $40 \times 40 \times 39$ image size. A quarter of these images are used as training images and the remaining are considered as testing images (see Table 2). Color images coded in the RGB color space are simulated from the hyperspectral images with CIE-1964 color matching functions and the D65 standard illumination.

HyTexiLa and SpecTex present a major drawback: the partitioning used to build these datasets consists of extracting training and testing sub-images from a same original image. However, such a partitioning, when it is combined with a classifier such as the nearest neighbor classifier, leads to biased classification results [26]. For this reason, a third challenging hyperspectral dataset built from the Timbers database is here proposed [32]. Timbers is a spectral image database of Nordic sawn timbers that has been acquired thanks to three hyperspectral cameras from board and crosscut samples analyzed in frozen, melted or room-dried conditions. 3 categories of wood species are available in this database: Birch (Betula sp.), Norway spruce (Picea abies) and Scots pine (Pinus sylvestris). The three Specim cameras, UV4E, V10E and N25E, measure reflectance in the 200–400, 400–1000 and 970–2500 nm wavelength ranges, respectively [33]. In this paper, we propose an original dataset of room-dried board samples acquired with the V10E camera. The information about the images considered in this dataset can be downloaded at `https://www-lisic.univ-littoral.fr/~porebski/`. The V10E camera is here chosen since it acquires images in the visible wavelength range, what is required to transform hyperspectral images to RGB ones. The spatial resolution of each image is 320×799 pixels. Like for HyTexiLa and SpecTex, we propose to consider a reduced number of $N_B = 30$ non-correlated spectral bands among the 1200 available ones (one band every forty bands). In order to have a suitable number of representative samples, 20 images are considered for each of the 3 categories. To ensure that images used for the training and the testing are less correlated as possible, 10 of these images are considered for the training and the others are used as testing images. Each of these images are then split up into 48 non-overlapping sub-images leading to $64 \times 64 \times 30$ image size (see Table 2). As for the SpecTex dataset, the RGB color images are simulated from the hyperspectral images with CIE-1964 color matching functions and the D65 standard illumination. Figure 2 illustrates samples represented by their simulated RGB images for each of the 3 texture classes. Although the number of classes is low, the textures of the different categories appear very close in this dataset. The classification is thus challenging due to the high inter-class similarity.

4.2 Specific descriptor setting

For HyTexiLa and SpecTex, the quantization level Q used to compute the reduced size chromatic co-occurrence matrices in the ICM descriptor is set to 16. This value enables ICM analysis to reach satisfying classification results while significantly reducing the processing time [26]. For the Timbers dataset, the sub-quantification of color components or spectral bands does not allow to well discriminate the texture classes since color or spectral ranges are very close from a class to another. For this reason, the

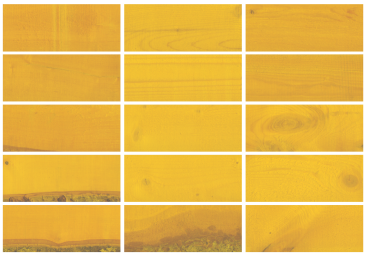

Figure 2: Timbers textured wood samples [32]. Each column illustrates some samples of one texture class [https://sites.uef.fi/spectral/spectral-image-database-of-nordic-sawn-timbers/].

quantization level for this dataset is set to 256 .

4.3 Considered color spaces

As previously seen, hyperspectral images can be easily converted to simulated color images coded in the RGB color space. There exist numerous color spaces that take into account different physical, physiologic and psycho-visual properties [4]. In this paper, $N_C = 10$ color spaces representative of the four color space families are considered for experiments: RGB and rgb, which belong to the primary space family, CIELAB, YCbCr and wb-rg-by, which are luminance-chrominance spaces, I1I2I3, which is an independent color component space, and HSV, HSI, HLS and I-HLS, which belong to the perceptual space family. A majority of perceptual spaces were chosen because these spaces are known to reach good classification accuracies [26].

4.4 Classification parameters

The images of the three hyperspectral texture databases are all assigned either to a training or a testing subset. In order to compare the MCC and MSB representations for supervised texture classification issues, the classification performance is assessed by following this holdout evaluation scheme. For this purpose, classification accuracies obtained with the proposed representations are evaluated by measuring the rate of well-classified testing images during the decision stage.

During the learning stage, the proposed embedded model use a k-fold evaluation method with $k = 3$ to determine the dimensionality of the selected feature sub-space.

The purpose of this paper being to show the contribution of different texture representations, independently of the considered classifier and its parameters, the nearest neighbor classifier is here considered. This classifier labels each testing or validation image with the closest match in the training set according to a similarity measure. When the ICM descriptor is considered, the nearest neighbor classifier is associated with the L1 distance and when LBP, ILBP and LCVBP descriptors are applied, the chi-square histogram distance metric is used as similarity measure [34]. Obviously, the classification results are expected to be improved by using more elaborated classifiers.

5 Results and discussions

5.1 Analysis of the results obtained with MSB and MCC representations

Table 3 presents the classification results reached with the three image datasets by the proposed MSB and MCC representations, according to the considered texture descriptors, the consideration of a marginal and/or an opponent component strategy (Mar, Opp or Mar+Opp), with and without selection. For each classification rate R, the number of considered features or histograms ($\hat{d}$ with selection or D without selection), with which testing images are classified, is given. For LBP, ILBP and LCVBP, $\hat{d}$ and D must be multiplied by the number of considered bins to have the final feature space dimension (256 for LBP and LCVBP, 511 for ILBP-Mar and 512 for ILBP-Mar+Opp). As done in [35], a global ranking metric allowing to compare the performance of each descriptor with others on all the considered databases is proposed. Since 14 descriptors and 3 datasets are considered, $3 \times 13 = 39$ comparisons are done for each descriptor and the score is the ratio of the wins over the total comparisons.

Table 3: Classification rates reached with the MSB and MCC representations. The values in bold correspond to the best accuracies reached for each dataset.

Descriptor	Hytexila				SpecTex				Timbers				Rank
	With selection		Without selection		With selection		Without selection		With selection		Without selection		
	R	$\hat{d}$	R	D	R	$\hat{d}$	R	D	R	$\hat{d}$	R	D	
MSB-LBP-Mar	93.13	26	93.13	27	98.11	30	98.17	39	58.61	26	58.47	30	12
MCC-LBP-Mar	97.80	22	96.91	30	97.47	28	97.40	30	65.69	24	65.76	30	9
MSB-LBP-Mar+Opp	98.76	728	98.76	729	99.33	1334	**99.38**	1521	79.10	897	79.24	900	1
MCC-LBP-Mar+Opp	97.66	88	97.80	90	97.95	87	97.97	90	68.75	87	68.47	90	5
MSB-ILBP-Mar	93.61	27	93.61	27	98.50	39	98.50	39	58.61	24	58.75	30	10
MCC-ILBP-Mar	96.84	28	97.05	30	98.10	30	98.10	30	66.32	28	65.76	30	8
MSB-ILBP-Mar+Opp	**99.11**	378	**99.11**	378	99.24	773	99.25	780	78.40	463	78.61	465	2
MCC-ILBP-Mar+Opp	98.49	59	98.35	60	98.42	60	98.42	60	69.03	60	69.03	60	3
MSB-LCVBP-Opp	97.12	108	96.29	351	98.67	193	98.70	741	67.99	433	68.33	435	4
MCC-LCVBP-Opp	96.77	28	96.63	30	97.55	23	97.55	30	66.32	30	66.32	30	12
MSB-ICM-Mar	89.84	17	93.82	378	92.10	15	96.18	546	82.15	6	70.42	420	14
MCC-ICM-Mar	97.18	24	97.53	420	94.89	86	95.05	420	73.26	5	74.38	420	11
MSB-ICM-Mar+Opp	96.77	10	95.05	5292	97.73	19	96.50	10920	**82.36**	22	73.26	6510	6
MCC-ICM-Mar+Opp	97.94	145	97.87	840	95.62	113	95.48	840	77.15	20	73.82	840	7

For HyTexiLa, SpecTex and Timbers, the best classification rates are respectively obtained with ILBP, LBP and ICM (99.11%, 99.38% and 82.36%) with a MSB representation including a marginal and opponent component strategy. Globally, whatever the considered descriptor X, MSB-X-Mar+Opp always outperforms MCC-X-Mar+Opp, which itself always surpasses MCC-X-Mar, which itself reaches better accuracy than MSB-X-Mar. It confirms the conclusions done in [8], where it has been shown that color imaging (MCC) reaches better accuracy than hyperspectral imaging (MSB) in a marginal context. However, when between component interactions are considered in addition to the within ones (Mar+Opp), this paper shows that hyperspectral imaging outperforms color imaging. This result is also checked with the LCVBP descriptor which uses only an opponent component strategy.

By analyzing Table 3, we can also notice that, when LBP, ILBP and LCVBP descriptors are considered, the selection neither clearly improves the classification rates, nor reduces the dimension of the feature space. The decision processing time being proportional to the number of considered features, these descriptors may involve an important on-line classification time. This conclusion was not expected since it is in contradiction with previous results where the histogram selection has significantly improved the accuracy while decreasing the decision processing time [5]. However, when ICM descriptor is used, the selection process allows to considerably reduce the dimension of the feature space. For example, the best rate reached with the Timbers dataset (82.36%) is obtained by only considering 22 well-suited Haralick features among 6510. It improves the accuracy obtained without selection of 9.1%. The MSB-ICM-Mar+Opp approach seems to be a good option to consider when low decision processing times are required.

5.2 Comparison with hand-designed color texture descriptors and CNN-based features

To enrich the discussion, the proposed MSB-X-Mar+Opp approach is compared with some typical hand-designed color texture descriptors and with CNN-based features. Five hand-designed descriptors computed from RGB color images have been evaluated: SWOBP [21], MCLBP [17], IOCLBP [23], OCLBP [3] and LCVBP [24]. As for our MCC and MSB representations, 8 neighbor pixels and 1 pixel radius define the neighborhood necessary to compute these descriptors. CNN-based features with five pre-

trained models (ResNet-50, ResNet-101, ResNet-152, VGG-16 and VGG-19) have also been added to the study [36, 37]. These models have been chosen since they allow to obtain the best accuracies on several color texture databases as shown in [27]. To obtain CNN-based feature classification results, each network is used as a generic feature extractor and the resulting features are passed on to a standard classifier (more information about the computation of the CNN-based features can be found in [27]). The classifier considered for these hand-designed color texture descriptors and CNN-based features is the nearest neighbor classifier associated with the chi-square distance.

Table 4 presents the classification rates reached with the three image datasets by the five hand-designed descriptors, the five CNN-based features and the proposed MSB representation when a marginal and opponent (Mar+Opp) or an opponent (Opp) strategy with selection is considered. The dimension of each descriptor and the global ranking metric are also presented.

We can notice that the proposed MSB-X-Mar+Opp representation (ranks 1 to 4) outperforms the CNN-based features (ranks 5 to 7 for the three best CNN) and the hand-designed descriptors (ranks 8 to 10 for the three best descriptors) computed from the RGB color space. This is particularly noticeable for the challenging Timbers dataset where the improvement reaches on average 13%. The feature space dimension is however high when LBP, ILBP or LCVPB are considered. On the contrary, the results reached with MSB-ICM-Mar+Opp representation offers a good compromise between accuracy and computation time since it outperforms the classification results obtained with the considered state of the art descriptors, while offering a very low dimensional feature space.

6 Conclusion

This study analyzes the contribution of hyperspectral and color imaging for texture classification in the visible spectrum. A comparison of MCC and MSB representations has been done in the context where both within and between component interactions are considered. The experiments carried out with several texture descriptors on three hyperspectral databases show that considering between component interactions in addition to the within ones significantly improves the classification rates when hyperspectral imaging with the MSB representation of textures is considered. A selection approach is however essential to reduce the dimension of the feature space and thus the decision processing times. The MSB-ICM-Mar+Opp descriptor is in that way a good option to consider since it outperforms state of the art hand-designed and CNN-based color texture descriptors both in accuracy and on-line classification computation time.

In this paper, we have also proposed an original dataset of room-dried board samples acquired by the V10E camera for Timbers. The textures of the different categories appearing very close, this dataset is particularly challenging due to the high inter-class similarity. It would be interesting for the future developments to consider other datasets extracted from crosscut samples and to analyze the textures in frozen or melted conditions.

References

[1] L. Liu, J. Chen, P. Fieguth, G. Zhao, R. Chellappa, M. Pietikäinen, From BoW to CNN: Two Decades of Texture Representation for Texture Classification, International Journal of Computer Vision 127 (1) (2019) 74–109. doi:10.1007/s11263-018-1125-z.

[2] F. Bianconi, A. Fernández, F. Smeraldi, G. Pascoletti, Colour and Texture Descriptors for Visual Recognition: A Historical Overview, Journal of Imaging 7 (11) (2021) 245. doi:10.3390/jimaging7110245.

[3] T. Mäenpää, M. Pietikäinen, Classification with color and texture: jointly or separately?, Pattern Recognition 37 (8) (2004) 1629–1640. doi:10.1016/j.patcog.2003.11.011.

Table 4: Comparison with state of the art approaches.

Descriptor	Hytexila		SpecTex		Timbers		Rank
	R	Dim	R	Dim	R	Dim	
MSB-LBP-Mar+Opp	98.76	728×256	**99.33**	1334×256	79.10	897×256	1
MSB-ILBP-Mar+Opp	**99.11**	378×512	99.24	773×512	78.40	463×512	2
MSB-LCVBP-Opp	97.12	108×256	98.67	193×256	67.99	433×256	3
MSB-ICM-Mar+Opp	96.77	10	97.73	19	**82.36**	22	4
ResNet-50-FC	97.73	2048	97.04	2048	65.63	2048	6
ResNet-101-FC	97.53	2048	97.10	2048	68.33	2048	5
ResNet-152-FC	98.15	2048	96.73	2048	67.71	2048	7
VGG-VD-16-FC	95.95	4096	96.73	4096	63.96	4096	12
VGG-VD-19-FC	96.09	4096	96.01	4096	64.24	4096	11
OCLBP	95.33	1536	98.30	1536	61.04	1536	8
IOCLBP	95.05	3069	98.38	3069	60.69	3069	9
MCLBP	94.92	531	97.63	531	64.51	531	10
LCVBP	94.02	1024	95.07	1024	60.42	1024	13
SWOBP	91.76	1048	93.53	1048	62.78	1048	14

[4] L. Busin, N. Vandenbroucke, L. Macaire, Color Spaces and Image Segmentation, in: Advances in Imaging and Electron Physics, Vol. 151, Elsevier, 2009, pp. 65–168. doi:10.1016/S1076-5670(07)00402-8.

[5] A. Porebski, V. T. Hoang, N. Vandenbroucke, D. Hamad, Multi-color space local binary pattern-based feature selection for texture classification, Journal of Electronic Imaging 27 (1) (2018) 011010. doi:10.1117/1.JEI.27.1.011010.

[6] S. Chindaro, K. Sirlantzis, F. Deravi, Texture classification system using colour space fusion, Electronics Letters 41 (10) (2005) 589. doi:10.1049/el:20050594.

[7] S. Banerji, A. Sinha, C. Liu, New image descriptors based on color, texture, shape, and wavelets for object and scene image classification, Neurocomputing 117 (2013) 173–185. doi:10.1016/j.neucom.2013.02.014.

[8] N. Vandenbroucke, A. Porebski, Multi Color Channel vs. Multi Spectral Band Representations for Texture Classification, in: ICPR International Workshops and Challenges, 2021, pp. 310–324. doi:10.1007/978-3-030-68790-8_25.

[9] R. Khelifi, M. Adel, S. Bourennane, Multispectral texture characterization: application to computer aided diagnosis on prostatic tissue images, EURASIP Journal on Advances in Signal Processing 2012 (1) (2012) 118. doi:10.1186/1687-6180-2012-118.

[10] H. Khan, S. Mihoubi, B. Mathon, J.-B. Thomas, J. Hardeberg, HyTexiLa: High Resolution Visible and Near Infrared Hyperspectral Texture Images, Sensors 18 (7) (2018) 2045. doi:10.3390/s18072045.

[11] R. J. Chu, N. Richard, F. Ghorbel, C. Fernandez-Maloigne, J. Y. Hardeberg, A Metrological Framework For Hyperspectral Texture Analysis Using Relative Spectral Difference Occurrence Matrix, in: 2019 10th WHISPERS Workshop, 2019, pp. 1–5. doi:10.1109/WHISPERS.2019.8921335.

[12] A. AlSuwaidi, B. Grieve, H. Yin, Spectral-texture approach to hyperspectral image analysis for plant classification with SVMs, in: 2017 IEEE International Conference on Imaging Sys-

tems and Techniques (IST), 2017, pp. 1–6. doi:10.1109/IST.2017.8261496.

[13] R. M. Haralick, K. Shanmugam, I. Dinstein, Textural Features for Image Classification, IEEE Transactions on Systems, Man, and Cybernetics SMC-3 (6) (1973) 610–621. doi:10.1109/TSMC.1973.4309314.

[14] T. Ojala, M. Pietikäinen, D. Harwood, A comparative study of texture measures with classification based on feature distributions, Pattern Recognition 29 (1) (1996) 51–59. doi:10.1016/0031-3203(95)00067-4.

[15] D. Bhattacharjee, H. Roy, Pattern of Local Gravitational Force (*PLGF*): A Novel Local Image Descriptor, IEEE Transactions on Pattern Analysis and Machine Intelligence 43 (2) (2021) 595–607. doi:10.1109/TPAMI.2019.2930192.

[16] M. Pietikäinen, G. Zhao, A. Hadid, T. Ahonen, Computer Vision Using Local Binary Patterns, no. 40 in Computational Imaging and Vision, Springer, 2011.

[17] X. Shu, Z. Song, J. Shi, S. Huang, X.-J. Wu, Multiple channels local binary pattern for color texture representation and classification, Signal Processing: Image Communication 98 (2021) 116392. doi:10.1016/j.image.2021.116392.

[18] C. Palm, Color texture classification by integrative Co-occurrence matrices, Pattern Recognition 37 (5) (2004) 965–976. doi:10.1016/j.patcog.2003.09.010.

[19] S. Fekri-Ershad, F. Tajeripour, Color texture classification based on proposed impulse-noise resistant color local binary patterns and significant points selection algorithm, Sensor Review 37 (1) (2017) 33–42. doi:10.1108/SR-07-2016-0120.

[20] C. Singh, E. Walia, K. P. Kaur, Color texture description with novel local binary patterns for effective image retrieval, Pattern Recognition 76 (2018) 50–68. doi:10.1016/j.patcog.2017.10.021.

[21] T. Song, J. Feng, S. Wang, Y. Xie, Spatially weighted order binary pattern for color texture classification, Expert Systems with Applications 147 (2020) 113167. doi:10.1016/j.eswa.2019.113167.

[22] T. Song, L. Xin, C. Gao, T. Zhang, Y. Huang, Quaternionic extended local binary pattern with adaptive structural pyramid pooling for color image representation, Pattern Recognition 115 (2021) 107891. doi:10.1016/j.patcog.2021.107891.

[23] F. Bianconi, R. Bello-Cerezo, P. Napoletano, F. Di Maria, Improved Opponent Colour Local Binary Patterns for Colour Texture Classification, in: Computational Color Imaging, 2017, pp. 272–281. doi:10.1007/978-3-319-56010-6_23.

[24] S. H. Lee, J. Y. Choi, Y. M. Ro, K. N. Plataniotis, Local Color Vector Binary Patterns From Multichannel Face Images for Face Recognition, IEEE Transactions on Image Processing 21 (4) (2012) 2347–2353. doi:10.1109/TIP.2011.2181526.

[25] A. Porebski, N. Vandenbroucke, L. Macaire, Neighborhood and Haralick Feature Extraction for Color Texture Analysis (2008) 6.

[26] A. Porebski, N. Vandenbroucke, L. Macaire, Supervised texture classification: color space or texture feature selection?, Pattern Analysis and Applications 16 (1) (2013) 1–18. doi:10.1007/s10044-012-0291-9.

[27] R. Bello-Cerezo, F. Bianconi, F. Di Maria, P. Napoletano, F. Smeraldi, Comparative Evaluation of Hand-Crafted Image Descriptors vs. Off-the-Shelf CNN-Based Features for Colour Texture Classification under Ideal and Realistic Conditions, Applied Sciences 9 (4) (2019) 738. doi:10.3390/app9040738.

[28] T. Hastie, R. Tibshirani, J. Friedman, Overview of Supervised Learning, Springer New York, 2009, Ch. Overview of Supervised Learning, pp. 9–41.

[29] G. Chandrashekar, F. Sahin, A survey on feature selection methods, Computers & Electrical Engineering 40 (1) (2014) 16–28. doi:10.1016/j.compeleceng.2013.11.024.

[30] M. Alimoussa, A. Porebski, N. Vandenbroucke, R. Thami, S. El Fkihi, Clustering-based Sequential Feature Selection Approach for High Dimensional Data Classification:, in: Proceedings of the 16th International Joint Conference on Computer Vision, Imaging and Computer Graphics Theory and Applications, 2021, pp. 122–132. doi:10.5220/0010259501220132.

[31] A. Mirhashemi, Introducing spectral moment features in analyzing the SpecTex hyperspectral texture database, Machine Vision and Applications 29 (3) (2018) 415–432. doi:10.1007/s00138-017-0892-9.

[32] T. Hirvonen, J. Orava, N. Penttinen, K. Luostarinen, M. Hauta-Kasari, M. Sorjonen, K.-E. Peiponen, Spectral image database for observing the quality of Nordic sawn timbers, Wood Science and Technology 48 (5) (2014) 995–1003. doi:10.1007/s00226-014-0655-y.

[33] T. Hirvonen, N. Penttinen, M. Hauta–Kasari, M. Sorjonen, K. Peiponen, A Wide Spectral Range Reflectance and Luminescence Imaging System, Sensors 13 (11) (2013) 14500–14510. doi:10.3390/s131114500.

[34] Q. Zhang, R. L. Canosa, A comparison of histogram distance metrics for content-based image retrieval, in: Imaging and Multimedia Analytics in a Web and Mobile World 2014, Vol. 9027, SPIE, 2014, pp. 154–162. doi:10.1117/12.2042359.

[35] M. Kas, I. E. khadiri, Y. El merabet, Y. Ruichek, R. Messoussi, Multi Level Directional Cross Binary Patterns, Engineering Applications of Artificial Intelligence 94 (2020) 103743. doi:10.1016/j.engappai.2020.103743.

[36] K. He, X. Zhang, S. Ren, J. Sun, Deep Residual Learning for Image Recognition, in: 2016 IEEE Conference on Computer Vision and Pattern Recognition (CVPR), 2016, pp. 770–778. doi:10.1109/CVPR.2016.90.

[37] K. Simonyan, A. Zisserman, Very Deep Convolutional Networks for Large-Scale Image Recognition (Apr. 2015). doi:10.48550/arXiv.1409.1556.